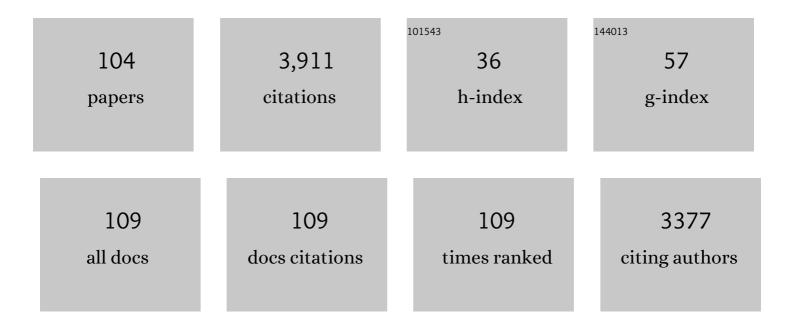
## Dirk Klaeschen

List of Publications by Year in descending order

Source: https://exaly.com/author-pdf/6240377/publications.pdf Version: 2024-02-01



#	Article	IF	CITATIONS
1	Structure of the Makran subduction zone from wide-angle and reflection seismic data. Tectonophysics, 2000, 329, 171-191.	2.2	212
2	The Calabrian Arc subduction complex in the Ionian Sea: Regional architecture, active deformation, and seismic hazard. Tectonics, 2011, 30, .	2.8	159
3	The S reflector west of Galicia (Spain): Evidence from prestack depth migration for detachment faulting during continental breakup. Journal of Geophysical Research, 1996, 101, 8075-8091.	3.3	149
4	High-resolution P-Cable 3D seismic imaging of gas chimney structures in gas hydrated sediments of an Arctic sediment drift. Marine and Petroleum Geology, 2010, 27, 1981-1994.	3.3	138
5	New seismic images of the Cascadia subduction zone from cruise SO108 — ORWELL. Tectonophysics, 1998, 293, 69-84.	2.2	100
6	Tectonic structure across the accretionary and erosional parts of the Japan Trench margin. Journal of Geophysical Research, 1994, 99, 22349-22361.	3.3	95
7	The Ionian and Alfeo–Etna fault zones: New segments of an evolving plate boundary in the central Mediterranean Sea?. Tectonophysics, 2016, 675, 69-90.	2.2	93
8	Extreme efficiency of mud volcanism in dewatering accretionary prisms. Earth and Planetary Science Letters, 2001, 189, 295-313.	4.4	90
9	Crustal structure of the central Sunda margin at the onset of oblique subduction. Geophysical Journal International, 2001, 147, 449-474.	2.4	88
10	Deep structure of the central Lesser Antilles Island Arc: Relevance for the formation of continental crust. Earth and Planetary Science Letters, 2011, 304, 121-134.	4.4	83
11	Seismic investigations of the O'Higgins Seamount Group and Juan Fernández Ridge: Aseismic ridge emplacement and lithosphere hydration. Tectonics, 2004, 23, n/a-n/a.	2.8	79
12	Fault-controlled hydration of the upper mantle during continentalÂrifting. Nature Geoscience, 2016, 9, 384-388.	12.9	75
13	Evolution of fluid expulsion and concentrated hydrate zones across the southern Hikurangi subduction margin, New Zealand: An analysis from depth migrated seismic data. Geochemistry, Geophysics, Geosystems, 2012, 13, .	2.5	74
14	Propagation of a lithospheric tear fault (STEP) through the western boundary of the Calabrian accretionary wedge offshore eastern Sicily (Southern Italy). Tectonophysics, 2013, 602, 141-152.	2.2	74
15	Crustal structure of the Java margin from seismic wide-angle and multichannel reflection data. Journal of Geophysical Research, 2002, 107, ETG 1-1.	3.3	67
16	Upward delamination of Cascadia Basin sediment infill with landward frontal accretion thrusting caused by rapid glacial age material flux. Tectonics, 2004, 23, n/a-n/a.	2.8	67
17	Ocean temperature and salinity inverted from combined hydrographic and seismic data. Geophysical Research Letters, 2010, 37, .	4.0	65
18	Non-Coulomb wedges, wrong-way thrusting, and natural hazards in Cascadia. Geology, 2001, 29, 379.	4.4	63

#	Article	IF	CITATIONS
19	On the origin of multiple BSRs in the Danube deep-sea fan, Black Sea. Earth and Planetary Science Letters, 2017, 462, 15-25.	4.4	59
20	The Mediterranean Ridge: A mass balance across the fastest growing accretionary complex on Earth. Journal of Geophysical Research, 2003, 108, .	3.3	58
21	Extreme crustal thinning in the south Porcupine Basin and the nature of the Porcupine Median High: implications for the formation of non-volcanic rifted margins. Journal of the Geological Society, 2004, 161, 783-798.	2.1	57
22	Gas-controlled seafloor doming. Geology, 2015, 43, 571-574.	4.4	56
23	Continental hyperextension, mantle exhumation, and thin oceanic crust at the continentâ€ocean transition, West Iberia: New insights from wideâ€angle seismic. Journal of Geophysical Research: Solid Earth, 2016, 121, 3177-3199.	3.4	53
24	Mass and fluid flux during accretion at the Alaskan margin. Bulletin of the Geological Society of America, 1998, 110, 468-482.	3.3	51
25	Internal configuration of the Levantine Basin from seismic reflection data (eastern Mediterranean). Earth and Planetary Science Letters, 2000, 180, 77-89.	4.4	49
26	The continental margin off Oregon from seismic investigations. Tectonophysics, 2000, 329, 79-97.	2.2	49
27	Movement along a low-angle normal fault: The S reflector west of Spain. Geochemistry, Geophysics, Geosystems, 2007, 8, n/a-n/a.	2.5	49
28	Midâ€depth internal wave energy off the Iberian Peninsula estimated from seismic reflection data. Journal of Geophysical Research, 2008, 113, .	3.3	49
29	A Miocene tectonic inversion in the Ionian Sea (central Mediterranean): Evidence from multichannel seismic data. Journal of Geophysical Research, 2011, 116, .	3.3	48
30	Seismic evidence for shallow gasâ€escape features associated with a retreating gas hydrate zone offshore west Svalbard. Journal of Geophysical Research, 2012, 117, .	3.3	47
31	Crustal structure along the EDGE transect beneath the Kodiak shelf off Alaska derived from OBH seismic refraction data. Geophysical Journal International, 1997, 130, 283-302.	2.4	44
32	From gradual spreading to catastrophic collapse – Reconstruction of the 1888 Ritter Island volcanic sector collapse from high-resolution 3D seismic data. Earth and Planetary Science Letters, 2019, 517, 1-13.	4.4	44
33	Evidence for active strike-slip faulting along the Eurasia-Africa convergence zone: Implications for seismic hazard in the southwest Iberian margin. Geology, 2012, 40, 495-498.	4.4	43
34	Frontal accretion along the western Mediterranean Ridge: the effect of Messinian evaporites on wedge mechanics and structural style. Marine Geology, 2002, 186, 59-82.	2.1	42
35	Active deformation in old oceanic lithosphere and significance for earthquake hazard: Seismic imaging of the Coral Patch Ridge area and neighboring abyssal plains (SW Iberian Margin). Geochemistry, Geophysics, Geosystems, 2013, 14, 2206-2231.	2.5	42
36	The impact of fluid advection on gas hydrate stability: Investigations at sites of methane seepage offshore Costa Rica. Earth and Planetary Science Letters, 2014, 401, 95-109.	4.4	42

#	Article	IF	CITATIONS
37	Earlyâ€stage rifting of the northern Tyrrhenian Sea Basin: Results from a combined wideâ€angle and multichannel seismic study. Geochemistry, Geophysics, Geosystems, 2013, 14, 3032-3052.	2.5	41
38	Insights into the emplacement dynamics of volcanic landslides from high-resolution 3D seismic data acquired offshore Montserrat, Lesser Antilles. Marine Geology, 2013, 335, 1-15.	2.1	39
39	Lower slope morphology of the Sumatra trench system. Basin Research, 2008, 20, 519-529.	2.7	37
40	Heterogeneous deformation in the Cascadia convergent margin and its relation to thermal gradient (Washington, NW USA). Tectonics, 2008, 27, .	2.8	37
41	Structure of the Kuril Trench from seismic reflection records. Journal of Geophysical Research, 1994, 99, 24173-24188.	3.3	36
42	Seismic images at the convergence zone from south of Cyprus to the Syrian coast, eastern Mediterranean. Tectonophysics, 2000, 329, 157-170.	2.2	36
43	Drivers of focused fluid flow and methane seepage at south Hydrate Ridge, offshore Oregon, USA. Geology, 2013, 41, 551-554.	4.4	35
44	The structure of the Africa-Anatolia plate boundary in the eastern Mediterranean. Tectonics, 2000, 19, 723-739.	2.8	34
45	Submarine gas seepage in a mixed contractional and shear deformation regime: Cases from the Hikurangi obliqueâ€subduction margin. Geochemistry, Geophysics, Geosystems, 2014, 15, 416-433.	2.5	33
46	Local seismic quantification of gas hydrates and BSR characterization from multi-frequency OBS data at northern Hydrate Ridge. Earth and Planetary Science Letters, 2007, 255, 414-431.	4.4	32
47	Two-stage growth of the Calabrian accretionary wedge in the Ionian Sea (Central Mediterranean): Constraints from depthâ€migrated multichannel seismic data. Marine Geology, 2012, 326-328, 28-45.	2.1	32
48	Crustal strain-dependent serpentinisation in the Porcupine Basin, offshore Ireland. Earth and Planetary Science Letters, 2017, 474, 148-159.	4.4	32
49	Seismic reflection along the path of the Mediterranean Undercurrent. Continental Shelf Research, 2009, 29, 1848-1860.	1.8	31
50	Opposing gradients of permanent strain in the aseismic zone and elastic strain across the seismogenic zone of the Kodiak shelf and slope, Alaska. Tectonics, 1999, 18, 248-262.	2.8	30
51	Anatomy of the western Java plate interface from depth-migrated seismic images. Earth and Planetary Science Letters, 2009, 288, 399-407.	4.4	30
52	Estimating movement of reflectors in the water column using seismic oceanography. Geophysical Research Letters, 2009, 36, .	4.0	30
53	Tectonic Controls on Gas Hydrate Distribution Off SW Taiwan. Journal of Geophysical Research: Solid Earth, 2019, 124, 1164-1184.	3.4	30
54	High-resolution, deep tow, multichannel seismic and sidescan sonar survey of the submarine mounds and associated BSR off Nicaragua pacific margin. Marine Geology, 2007, 241, 33-43.	2.1	28

#	Article	IF	CITATIONS
55	Effect of seismic source bandwidth on reflection sections to image water structure. Geophysical Research Letters, 2009, 36, .	4.0	26
56	Gas hydrate distribution and hydrocarbon maturation north of the Knipovich Ridge, western Svalbard margin. Journal of Geophysical Research: Solid Earth, 2016, 121, 1405-1424.	3.4	26
57	Relation between the Subducting Plate and Seismicity Associated with the Great 1964 Alaska Earthquake. Pure and Applied Geophysics, 1999, 154, 575-591.	1.9	23
58	<i>P</i> and <i>S</i> wave velocity measurements of water-rich sediments from the Nankai Trough, Japan. Journal of Geophysical Research: Solid Earth, 2014, 119, 787-805.	3.4	23
59	Splay fault branching from the <scp>H</scp> ikurangi subduction shear zone: Implications for slow slip and fluid flow. Geochemistry, Geophysics, Geosystems, 2016, 17, 5009-5023.	2.5	23
60	Resolving the fine-scale velocity structure of continental hyperextension at the Deep Galicia Margin using full-waveform inversion. Geophysical Journal International, 2018, 212, 244-263.	2.4	23
61	Characterization of the submesoscale energy cascade in the Alboran Sea thermocline from spectral analysis of highâ€resolution MCS data. Geophysical Research Letters, 2016, 43, 6461-6468.	4.0	22
62	Seismic Oceanography in the Tyrrhenian Sea: Thermohaline Staircases, Eddies, and Internal Waves. Journal of Geophysical Research: Oceans, 2017, 122, 8503-8523.	2.6	22
63	Linked halokinesis and mud volcanism at the Mercator mud volcano, Gulf of Cadiz. Journal of Geophysical Research, 2011, 116, .	3.3	21
64	Heat flow in the southern Chile forearc controlled by large-scale tectonic processes. Geo-Marine Letters, 2014, 34, 185-198.	1.1	21
65	Estimating internal wave spectra using constrained models of the dynamic ocean. Geophysical Research Letters, 2009, 36, .	4.0	19
66	Crustal thinning in the northern Tyrrhenian Rift: Insights from multichannel and wideâ€angle seismic data across the basin. Journal of Geophysical Research: Solid Earth, 2014, 119, 1655-1677.	3.4	19
67	Deep structure of the Porcupine Basin from wide-angle seismic data. Petroleum Geology Conference Proceedings, 2018, 8, 199-209.	0.7	19
68	Ionian Abyssal Plain: a window into the Tethys oceanic lithosphere. Solid Earth, 2019, 10, 447-462.	2.8	19
69	Insights into active deformation in the Gulf of Cadiz from new 3-D seismic and high-resolution bathymetry data. Geochemistry, Geophysics, Geosystems, 2011, 12, n/a-n/a.	2.5	18
70	Gas migration through Opouawe Bank at the Hikurangi margin offshore New Zealand. Geo-Marine Letters, 2016, 36, 187-196.	1.1	18
71	Morphostructure, tectonoâ€sedimentary evolution and seismic potential of the Horseshoe Fault, <scp>SW</scp> Iberian Margin. Basin Research, 2018, 30, 382-400.	2.7	18
72	Crustal structure of the central Costa Rica subduction zone: implications for basal erosion from seismic wide-angle data. Geophysical Journal International, 2009, 178, 1112-1131.	2.4	17

#	Article	IF	CITATIONS
73	Effect of bandwidth on seismic imaging of rotating stratified turbulence surrounding an anticyclonic eddy from field data and numerical simulations. Geophysical Research Letters, 2009, 36, .	4.0	17
74	High resolution seismic imaging of the ocean structure using a small volume airgun source array in the Gulf of Cadiz. Geophysical Research Letters, 2009, 36, .	4.0	17
75	Tectonic regime of the southern Kurile Trench as revealed by multichannel seismic lines. Tectonophysics, 1995, 241, 259-277.	2.2	16
76	Subduction system variability across the segment boundary of the 2004/2005 Sumatra megathrust earthquakes. Earth and Planetary Science Letters, 2013, 365, 108-119.	4.4	16
77	From Continental Hyperextension to Seafloor Spreading: New Insights on the Porcupine Basin From Wideâ€Angle Seismic Data. Journal of Geophysical Research: Solid Earth, 2018, 123, 8312-8330.	3.4	16
78	A first estimation of gas hydrates offshore Patagonia (Chile). Marine and Petroleum Geology, 2018, 96, 232-239.	3.3	15
79	Subducted sediments, upper-plate deformation and dewatering at New Zealand's southern Hikurangi subduction margin. Earth and Planetary Science Letters, 2020, 530, 115945.	4.4	15
80	Mass wasting at the base of the south central Chilean continental margin: the Reloca Slide. Advances in Geosciences, 0, 22, 155-167.	12.0	15
81	New insights into geology and geochemistry of the Kerch seep area in the Black Sea. Marine and Petroleum Geology, 2020, 113, 104162.	3.3	13
82	Detachment tectonics at Mid-Atlantic Ridge 26°N. Scientific Reports, 2019, 9, 11830.	3.3	12
83	Seismic reflection imaging of mixing processes in Fram Strait. Journal of Geophysical Research: Oceans, 2015, 120, 6884-6896.	2.6	11
84	A Possible Source Mechanism of the 1946 Unimak Alaska Far-Field Tsunami: Uplift of the Mid-Slope Terrace Above a Splay Fault Zone. Pure and Applied Geophysics, 2016, 173, 4189-4201.	1.9	11
85	An automated ray method for diffraction modelling in complex media. Geophysical Journal International, 1994, 116, 23-38.	2.4	10
86	Relationship Between Subduction Erosion and the Upâ€Dip Limit of the 2014 Mw 8.1 Iquique Earthquake. Geophysical Research Letters, 2021, 48, e2020GL092207.	4.0	10
87	Stochastic Heterogeneity Mapping around a Mediterranean salt lens. Ocean Science, 2010, 6, 423-429.	3.4	9
88	Elongate fluid flow structures: Stress control on gas migration at Opouawe Bank, New Zealand. Marine and Petroleum Geology, 2018, 92, 913-931.	3.3	9
89	The case against porosity change: Seismic velocity decrease at the toe of the Oregon accretionary prism. Geology, 1995, 23, 827.	4.4	8
90	Geophysical evidence for late stage magmatism at the central Ninetyeast Ridge, Eastern Indian Ocean. Marine Geophysical Researches, 2001, 22, 225-234.	1.2	8

#	Article	IF	CITATIONS
91	Dual-vergence structure from multiple migration of widely spaced OBSs. Tectonophysics, 2017, 718, 45-60.	2.2	7
92	Wide-angle vibroseis data from the western Rhenish Massif. Tectonophysics, 1990, 173, 83-93.	2.2	6
93	Tectonic framework of the mud mounds, associated BSRs and submarine landslides, offshore Nicaragua Pacific margin. Journal of the Geological Society, 2008, 165, 167-176.	2.1	6
94	Margin architecture and seismic attenuation in the central Costa Rican forearc. Marine Geology, 2010, 276, 30-41.	2.1	5
95	Subducting oceanic basement roughness impacts on upper-plate tectonic structure and a backstop splay fault zone activated in the southern Kodiak aftershock region of the Mw 9.2, 1964 megathrust rupture, Alaska. , 2021, 17, 409-437.		5
96	Marine forearc structure of eastern Java and its role in the 1994 Java tsunami earthquake. Solid Earth, 2021, 12, 2467-2477.	2.8	5
97	AVA analysis in the eastern Mediterranean. Physics and Chemistry of the Earth, 1999, 24, 467-474.	0.6	4
98	Megathrust reflectivity reveals the updip limit of the 2014 Iquique earthquake rupture. Nature Communications, 2022, 13, .	12.8	4
99	Comparison of 2-D and 3-D full waveform inversion imaging using wide-angle seismic data from the Deep Galicia Margin. Geophysical Journal International, 2021, 227, 228-256.	2.4	3
100	AVA analysis reveals in situ sediment diagenesis at the Costa Rican décollement. Sedimentary Geology, 2007, 196, 269-277.	2.1	2
101	Potential of 3â€Ð vertical seismic profiles to characterize seismogenic fault zones. Geochemistry, Geophysics, Geosystems, 2008, 9, .	2.5	2
102	Insights Into Exhumation and Mantle Hydration Processes at the Deep Galicia Margin From a 3D Highâ€Resolution Seismic Velocity Model. Journal of Geophysical Research: Solid Earth, 2022, 127, .	3.4	1
103	Characterization of thermohaline staircases in the Tyrrhenian Sea using stochastic heterogeneity mapping. Proceedings of Meetings on Acoustics, 2013, , .	0.3	0
104	Relation between the Subducting Plate and Seismicity Associated with the Great 1964 Alaska Earthquake. , 1999, , 575-591.		0